RSC Advances

PAPER

View Article Online
View Journal | View Issue

Cite this: *RSC Adv.*, 2017, **7**, 10124

Dispersion and soap-free emulsion polymerization of *tert*-butyl acrylate with the living character and controlled particle size mediated by cobalt porphyrin

Huanqin Zhao, Baolong Wang, Qingpan Li, Liying Wang,* Junmin Sun, Yongfeng Zhang, Lichun Ji and Zhenzhu Cao

Received 17th December 2016
Accepted 21st January 2017

DOI: 10.1039/c6ra28325j

rsc.li/rsc-advances

Living radical polymerization (LRP) of *tert*-butyl acrylate (*t*BA) was carried out *via* dispersion and soap-free emulsion polymerization mediated by cobalt porphyrin [cobalt tetramethoxyphenylporphyrin, (TMOP)Co(II)] and initiated by 2,2′-azobis[2-(2-imidazolin-2-yl)propane] dihydrochloride (VA-044), respectively. The living character was demonstrated by the linear first-order kinetics with different feeding ratios of *t*BA and (TMOP)Co(II) and a linear increase in the number-average molecular weight was observed with the monomer conversion, as well as the relatively narrow polydispersity. However, only few studies have been reported on (TMOP)Co(II) mediating a living radical dispersion or soap-free emulsion polymerization of *t*BA. In addition, the obtained poly(*tert*-butyl acrylate) (P*t*BA) particles exhibited good uniformity and controlled particle size whether in the dispersion system or in the soap-free emulsion polymerization.

Introduction

Dispersion and emulsion polymerization, which are radical polymerization techniques, have been used for coatings, adhesives, inks, and many industrial applications.[1] Dispersion and emulsion polymerization technologies possess unique advantages, such as faster polymerization rate, polymers with high molecular weight, good heat transfer, low viscosity, and direct application.[2,3] However, they also have some drawbacks including the contamination of product with additives and no easy control in the case of hydrophilic monomers and polymer structures (composition, shape, topology, and functionality).[4,5] To overcome these disadvantages, the living/controlled radical polymerization (L/CRP) was developed,[6,7] allowing the designing of specialty polymers such as macromonomers, functional polymers, block polymers, and graft (comb or star) polymers. However, only few studies have been reported on the LRP of *tert*-butyl acrylate in the dispersion system and soap-free emulsion polymerization. The LRP system could be obtained *via* reversible addition fragmentation transfer (RAFT),[8,9] atom transfer radical polymerization (ATRP),[10,11] nitroxide-mediated radical polymerization (NMRP),[12,13] and organometallic-mediated radical polymerization (OMRP).[14,15] Particularly, cobalt complex-mediated radical polymerization (CMRP) represents one of the most successful and efficient OMRPs.[16] This process relies on the temporary deactivation of the propagating radicals by cobalt(II) complexes with the formation of organocobalt(III) dormant species. Since the Co–C bond cleavage can be achieved under mild conditions, thermal-initiated LRP mediated by organocobalt porphyrins has recently received significant attention due to its inherent advantages including environmentally benign reagents, low activation energy, simple operation processes, and mild polymerization conditions.[17,18] Tetramesityl porphyrin cobalt ((TMP)Co(II)) was used to mediate the LRP of acrylates by Wayland and his coworkers for many years and it provided rather low polydispersity homopolymers and several copolymers.[17–22] Very large steric requirements and restrictive solubility characteristics for (TMP)Co limit the scope of monomers that can be incorporated into block copolymers. The formation and application of brominated and sulfonated cobalt porphyrin complexes allowed LRP to speed up the polymerization of acrylates[18] and to mediate the polymerization of acrylic acid in an aqueous medium,[17] respectively. In addition, cobalt porphyrin substituted by three mesityl groups and one phenyl group that has a long chain alcohol in the *para*-position (TMP-OH) was designed to increase the solubility in different classes of solvents, which has been applied in the radical polymerizations of various acrylates and acrylamides[23–25] mediated by (TMP-OH)Co and initiated by azobis(isobutyronitrile) (AIBN) in benzene and methanol. In addition, tertiary butyl acrylate, which was only poorly controlled by (TMP)Co,[20,21] was observed to be well controlled by (TMP-OH)Co in both benzene and methanol. However, the abovementioned LRP reactions were performed in the solution polymerization

School of Chemical Engineering, Inner Mongolia University of Technology, Institute of Coal Conversion and Cyclic Economy, Huhhot, 010051, People's Republic of China. E-mail: wangliying7704@163.com

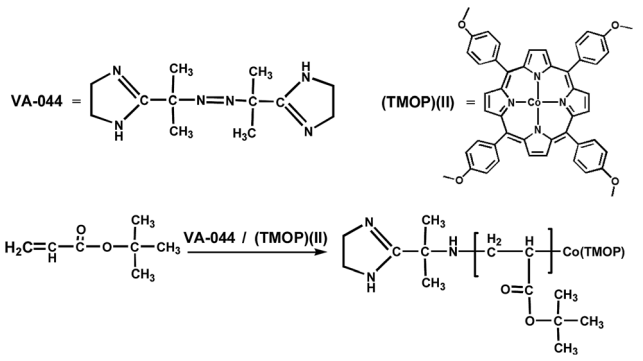

Scheme 1 Polymerization of *tert*-butyl acrylate.[8]

process, and to date, little research has been reported on the LRP of *tert*-butyl acrylate in the dispersion system and soap-free emulsion polymerization *via* CMRP.

Recently, we reported the dispersion polymerization of acrylamide (AM) mediated by (TMOP)Co(II).[26] The synthesized poly (AM) had narrow polydispersity values ($M_w/M_n = 1.09$–1.35) and the corresponding molecular weight (M_n) linearly increased with the monomer conversion. However, the conversion was relatively low (~40%). Herein, the dispersion and soap-free emulsion polymerization of *tert*-butyl acrylate were applied to obtain P*t*BA with low-molecular weight (less than 100 000 g mol^{-1}) and relatively narrow molecular distribution. These polymerizations obtained *via* CMRP were mediated by (TMOP)Co(II) and initiated by VA-044 in an environmentally friendly process and the conversion reached about 60–72% with the living character (Scheme 1).

Experimental

Materials

tert-Butyl acrylate (*t*BA, Aladdin, 99%) was filtered through neutral alumina, distilled under reduced pressure, and stored in the refrigerator before use. Cobalt tetramethoxyphenylporphyrin [(TMOP)Co(II), Alfa Aesar, 98%], polyvinylpyrrolidone (PVP, M_n = 10 000, Aladdin Biological and Chemical Reagent Co., Ltd, Shanghai, China), sodium chloride (NaCl, Tianjin Yongsheng Fine Chemical Co, Ltd., Tianjin, China, 99.5%), sodium dodecyl sulfate (SDS, Aladdin, 97%), hydroquinone (Aladdin, 99%) and 2,2′-azobis[2-(2-imidazolin-2-yl)propane] dihydrochloride (VA-044, Shanghai Yuanye Bio-Technology Co., Ltd., Shanghai, China) were used without further purification. All other reagents were used as received if not otherwise mentioned.

Preparation of the polymer

The polymer was prepared by the soap-free emulsion polymerization, which was carried out in a 100 mL four-necked flask with a stirrer, a reflux condenser, a thermometer, and a nitrogen inlet tube. First, water phase, comprising NaCl (0.05 g), SDS (0.006 mol L^{-1}) (the concentration was less than its critical micelle concentration (CMC)), and deionized water, was added to a 50 mL centrifuge tube and thoroughly dissolved. Moreover, monomer phase, including 3 g *t*BA, 0.005 g (TMOP)Co(II) (molar ratio with 3700/1), and ethanol was ultrasonicated for 10 min, and then added to the medium. The ingredients of the recipe (mixture of water phase and monomer phase) were mixed using a mini whirlpool mixer to form a homogeneous water/oil (W/O) emulsion at ambient temperatures. Finally, all the ingredients were put into the abovementioned 100 mL four-necked round-bottom flask, which was placed in a thermostated water bath at 25 °C, purged with nitrogen to remove O_2, capped, and sealed. The polymerization was initiated by injecting the VA-044 initiator into the system. The reaction mixture was mechanically stirred at 150 rpm for 3 h at 50 °C under a nitrogen atmosphere. At regular time intervals, an aliquot was taken for gravimetric conversion measurements and the reaction was stopped by exposure to air and dropwise addition of 5% hydroquinol inhibitor.

In the same manner, the polymer was also prepared by the dispersion polymerization, using the same abovementioned instruments. All the ingredients, such as monomer, PVP, alcohol, and deionized water were added to the 100 mL four-necked flask. After purging with nitrogen for 30 min, polymerization was initiated by adding (TMOP)Co(II) and VA-044 into the system. The obtained homogeneous emulsion was first precipitated in methanol and deionized water (1 : 1 v/v), and then the polymers were prepared by centrifugation and drying under vacuum.

Polymer characterization

The ^{1}H NMR spectrum of polymer was obtained in $CDCl_3$ using a Bruker (500 MHz ^{1}H) NMR spectrometer (Bruker Corporation, Bremen, Germany). The morphologies of the P*t*BA particles were investigated using a Quanta-250 scanning electron microscope (FEI Corporation, America) and Olympus BX53 optical microscope (Olympus Corporation, Japan). Analytical gel permeation chromatography (GPC) was performed using an Agilent 1200 series system equipped with a VARIAN Polar Gel-M column (300 × 7.5 mm), an Iso Pump (G1310A), a UV detector at 254 nm, and a differential refractive index detector (RI). The relative molecular weight (M_n) and polydispersity index (PDI) of the polymer were determined using the RI detector. *N*,*N*-Dimethyformamide (DMF) was used as the eluent at 50 °C with a flow rate of 1 mL min^{-1}. Nine narrowly distributed poly (MMA) samples (molecular weight range of 690–1 944 000 g mol^{-1}, from Poly Laboratories) were used as the calibration standards for the system. The diameters of P*t*BA particles were measured using the Image-Pro Plus 6.2 software[27] and a ZEN3690 light scattering particle size analyzer (Malvern Corporation, UK).

Results and discussion

Cobalt porphyrin (TMOP)Co(II) was tested as to whether it can mediate the dispersion polymerization of *t*BA in alcohol/water at 50 °C, as outlined in Table 1. The semilogarithmic plots for these polymerizations are shown in Fig. 1. When the conversion

reached a certain value with the living character, the rate of polymerization slightly decreased. Similar results have previously been reported for the radical polymerization of methyl acrylate with ((TMP)Co(II))[21] as well as acrylamide polymerization with RAFT inverse miniemulsion.[8] In the early stage of the polymerization (within 30–70 min, conversion < 60.0%), the plot exhibits an almost straight line, which indicates that the dispersion of the polymerization of *t*BA follows first-order kinetics, also indicating the generation of a constant concentration of growing radicals during this stage.[24] However, the first-order kinetic plot becomes increasingly nonlinear after 70 min. It is probable that there were two chief causes. First, the thermal-induced LRP mediated by organocobalt porphyrins probably proceeded through a degenerate transfer (DT) pathway;[21] the concentration of radicals for a DT process is primarily determined by the concentration of the external radical source (VA-044), which was excessive relative to the content of (TMOP)Co(II). When the influx of new radicals from VA-044 ended and the polymerization reaction reverted to a slower RT pathway, the rates of polymerization mainly controlled by the radical were maintained at a low concentration by a quasi-equilibrium between (TMP)CoII$^{\bullet}$ and organocobalt(III) species, which was formed by (TMP)CoII$^{\bullet}$ and propagating radicals in the solution. First, Fig. 1 also illustrates that on maintaining the amount of (TMOP)Co(II) and keeping the monomer concentration constant, the rate of polymerization decreased with the $[t\text{BA}]_0/[\text{Co}]_0$ molar ratio, which was order with the concentration of VA-044 which generated organic radical captured monomers forming a propagating chain radical at the first stage of polymerization, where the mechanism of DT is to occupy a significant place. Second, the polymerization at the high conversion region was affected by the diffusion-controlled phenomena. The polymerization was carried out in a highly concentrated solution after 70 min (conversion achieved was 60.0%) and the viscosity of the solution greatly increased, which led to the difficulty in monomer diffusion. Thus, the kinetic rate constant values moderately decreased as the polymerization proceeded.[28] The dispersion polymerization of *t*BA conducted with the same amount of

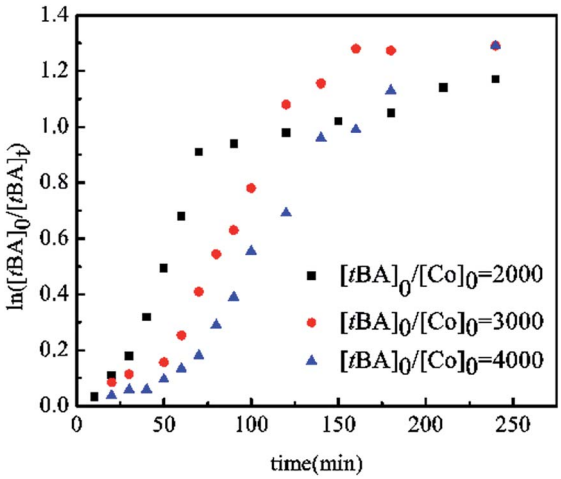

Fig. 1 Kinetics for the dispersion polymerization of *t*BA with different feeding ratio of *t*BA and (TMOP)Co(II) (conditions: monomer, 10 wt%; PVP, 20 wt%; $V_{\text{EtOH}}/V_{\text{H}_2\text{O}}$ = 5/5; temperature, 50 °C).

(TMOP)Co(II) and VA-044, as well as different amounts of monomer, shows that the rate of the polymerization is affected by the molar ratio $[t\text{BA}]_0/[\text{Co}]_0$. Different $[t\text{BA}]_0/[\text{Co}]_0$ molar ratios ranging from 2000/1 to 4000/1 indicated that LRP of *t*BA mediated by (TMOP)Co(II) in alcohol/water could be controlled over a wide range of $[t\text{BA}]_0/[\text{Co}]_0$ molar ratios without an apparent induction period. The apparent rate constant values for the polymerization were determined to be 1.82×10^{-2}, 1.31×10^{-2}, and 1.05×10^{-2} min^{-1} (corresponding to 2000/1, 3000/1, and 4000/1 ratios, respectively), which is the same order for the concentration of (TMOP)Co(II). Thus, high concentration of Co catalysts seem to be most effective.[29–32] However, the molecular weight distribution of the resulting P*t*BA is quite broad (PDI > 1.5).[33,34] The poor control for the dispersion polymerization of *t*BA that resulted from (TMOP)Co(II) with its very large steric structure restricted its solubility in alcohol/water, and the combined steric demands from the four mesityl groups of (TMOP)Co(II) and the *tert*-butyl group of *t*BA could

Table 1 Dispersion polymerizations of *t*BA mediated by (TMOP)Co(II)[a]

Run	$[t\text{BA}]_0/[\text{Co}]_0/[\text{VA-044}]_0$[a]	Time (min)	Conv.[b] (%)	$M_{\text{n,th}}$ ($\times 10^4$)[c]	$M_{\text{n,GPC}}$ ($\times 10^4$)[d]	M_w/M_n
1	2000/1/3	50	39.0	9.90	5.88	1.69
2	2000/1/3	60	49.3	12.6	6.95	3.19
3	2000/1/3	70	60.0	15.4	7.45	3.21
4	3000/1/3	60	22.4	8.60	5.24	1.77
5	3000/1/3	80	42.0	16.1	5.58	1.75
6	3000/1/3	180	72.0	27.7	6.21	1.54
7	4000/1/3	100	42.6	21.8	4.43	2.39
8	4000/1/3	120	50.0	25.6	4.98	1.39
9	4000/1/3	160	63.0	32.2	8.52	1.60
10	4000/1/3	180	67.8	34.7	10.6	1.76

[a] $[t\text{BA}]_0$ = 10%; [Co] = [(TMOP)Co(II)]; PVP, 20 wt%; $V_{\text{EtOH}}/V_{\text{H}_2\text{O}}$ = 5/5; temperature, 50 °C. [b] The monomer conversion was determined by gravimetric analysis. [c] $M_{\text{n,th}} = M_{\text{w}(t\text{BA})} \times$ ratio $\times$ conv (%). [d] Determined by gel permeation chromatography (GPC) calibrated by poly(MMA) standards.

lead to the decrease of the bond dissociation enthalpy of Co–C.[23]

Taking the [AM]/[Co] molar ratio of 4000/1 (Fig. 2) as an example, the experimental molecular weight of the P*t*BA linearly increased with monomer conversion. As shown in Fig. 3, GPC traces for the polymerization of *t*BA took the form of single-peak curves and are reasonably symmetrical. These results demonstrated the living character and controllability of (TMOP)Co(II) in the dispersion polymerization of *t*BA.[17] In addition, the molecular weight slightly deviated from the theoretical molecular weight of the P*t*BA (Table 1). This could be due to the system not fulfilling the assumption of complete conversion of cobalt(II) into organocobalt(III) in alcohol/water solution.[35,36]

For the dispersion polymerization of *t*AB, PVP containing high binding affinity with polar solvents was chosen as the stabilizer for the synthesis of monodispersed latex particles.[37] PVP concentration was also an important parameter that could influence the kinetics and subsequently the morphology of the polymer particles. To determine this effect, the reaction was carried out at 10%, 15%, 20%, and 25% keeping the monomer concentration constant, and the morphology of the particles obtained from these reactions are presented in Table 2 and Fig. 4. The data indicated that the particle size decreased with the increase in the amount of PVP. It was probable that the higher PVP concentration can increase both the adsorption rate of PVP and the viscosity of the continuous phase. These would reduce the extent of aggregation, resulting in smaller particles and a shorter particle formation stage.[38] Experiments were also carried out to investigate the effect of the feeding molar ratio of $[t\text{BA}]_0/[\text{Co}]_0$ on the particles. As shown in Fig. 5 and Table 3, the particle size decreases from 0.23 to 0.16 μm with the increasing feeding ratio of $[t\text{BA}]_0$ and $[\text{Co}]_0$ in the range from 2000/1 to 4000/1. This experiment was set at keeping the mass of VA-044, (TMOP)Co(II), and PVP constant, as well as keeping the mass concentration of the monomer at 10%. The concentration of the initiator (VA-044) increased with the decreasing feeding ratio of *t*BA and (TMOP)Co(II). Increasing the initiator concentration caused increase in the instantaneous concentration of the oligomeric radicals, which in turn increased the rate of association of the oligomers and/or the coagulation rate of the unstable nuclei to form larger permanent particle nuclei and, therefore, a larger final particle size.[39]

Furthermore, we also conducted the soap-free emulsion polymerization of *t*BA mediated by (TMOP)Co(II) with VA-044 acting as the initiator (Table 4). To evaluate the living character of these polymerization processes, the kinetic rate plots

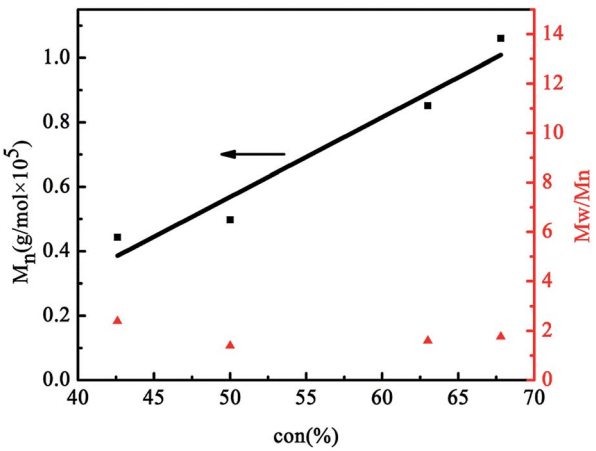

Fig. 2 Evolution of molar mass and polydispersity *versus* *t*BA conversion (conditions: $[t\text{BA}]_0/[\text{Co}]_0/[\text{VA-044}]_0$ = 4000/1/3; monomer, 10 wt%; PVP, 20 wt%; $V_{\text{EtOH}}/V_{\text{H}_2\text{O}}$ = 5/5; temperature, 50 °C).

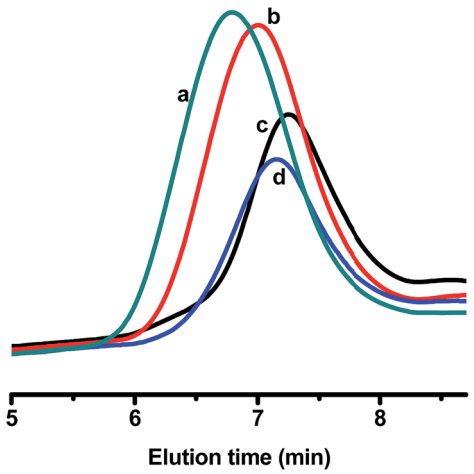

Fig. 3 GPC trace of P*t*BA: (a) Con. = 67.8%, $M_n = 10.6 \times 10^4$; (b) Con. = 63.0%, $M_n = 8.52 \times 10^4$; (c) Con. = 50.0%, $M_n = 4.98 \times 10^4$; and (d) Con. = 42.6%, $M_n = 4.43 \times 10^4$ (conditions: $[t\text{BA}]_0/[\text{Co}]_0/[\text{VA-044}]_0$ = 4000/1/3; monomer, 10 wt%; PVP, 20 wt%; $V_{\text{EtOH}}/V_{\text{H}_2\text{O}}$ = 5/5).

Table 2 Effect of different amounts of PVP on P*t*BA particle size

$[t\text{BA}]_0/[\text{Co}]_0/[\text{VA-044}]$	PVP (wt%)	D_{max} (μm)	D_{min} (μm)	D_{mean} (μm)
3000/1/3	10	0.76	0.41	0.59
3000/1/3	15	0.31	0.17	0.24
3000/1/3	20	0.30	0.17	0.22
3000/1/3	25	0.26	0.12	0.19

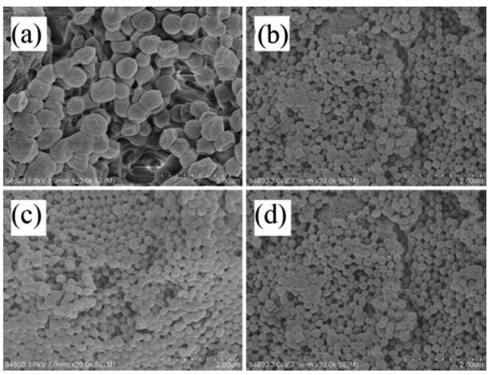

Fig. 4 Morphologies of P*t*BA particles at (a) PVP, 10 wt%; (b) PVP, 15 wt%; (c) PVP, 20 wt%; and (d) PVP, 25 wt% (conditions: $[t\text{BA}]_0/[\text{Co}]_0$ = 3000/1; monomer, 10 wt%; $V_{\text{EtOH}}/V_{\text{H}_2\text{O}}$ = 5/5; temperature, 50 °C).

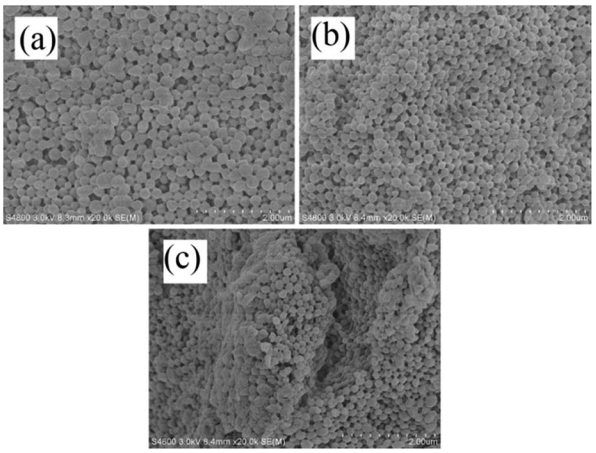

Fig. 5 Morphologies of the P*t*BA particles at (a) $[t\text{BA}]_0/[\text{Co}]_0 = 2000/1$; (b) $[t\text{BA}]_0/[\text{Co}]_0 = 3000/1$; and (c) $[t\text{BA}]_0/[\text{Co}]_0 = 4000/1$ (conditions: monomer, 10 wt%; PVP, 20 wt%; $V_{\text{EtOH}}/V_{\text{H}_2\text{O}} = 5/5$; temperature, 50 °C).

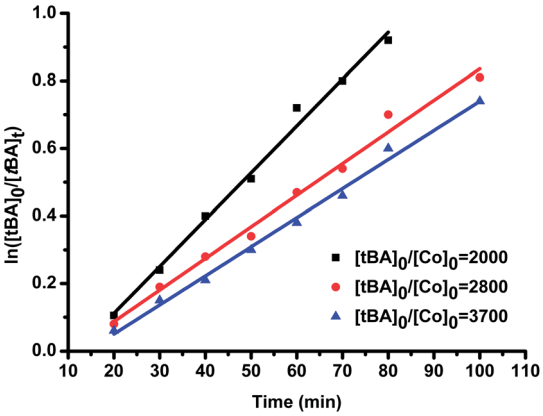

Fig. 6 Kinetics for the soap-free emulsion polymerization of *t*BA with different feeding ratio of *t*BA and (TMOP)Co(II) (black squares: slope = 1.39×10^{-2}; $R = 0.9911$; red circles: slope = 9.36×10^{-3}; $R = 0.9880$; blue triangles: slope = 8.62×10^{-3}; $R = 0.9929$; conditions: monomer, 10 wt%; c(SDS) = 0.006 mol L^{-1}; m(NaCl) = 0.05 g; $V_{\text{EtOH}}/V_{\text{H}_2\text{O}} = 2/8$; temperature, 50 °C).

Table 3 Effect of different feeding ratio of $[t\text{BA}]_0/[\text{Co}]_0$ on the P*t*BA particle sizes

$[t\text{BA}]_0/[\text{Co}]_0/[\text{VA-044}]$	PVP (wt%)	D_{max} (μm)	D_{min} (μm)	D_{mean} (μm)
2000/1/3	20	0.35	0.18	0.23
3000/1/3	20	0.29	0.17	0.22
4000/1/3	20	0.21	0.12	0.16

for the polymerization of *t*BA were studied (Fig. 6). The soap-free emulsion polymerization of *t*BA, almost without induction period, was observed to proceed with the linear first-order kinetics, indicating the generation of a constant concentration of growing radicals during the period of relatively fast polymerization. On keeping the amount of (TMOP)Co(II) and the monomer concentration constant, the rate of polymerization decreased with the $[t\text{BA}]_0/[\text{Co}]_0$ molar ratio, which is the same order for the concentration of (TMOP)Co(II).[29–32] Indeed, the apparent rate constant values were 1.39×10^{-2}, 9.36×10^{-3}, and 8.62×10^{-3} min^{-1}, corresponding to 2000/1, 2800/1, and 3700/1, respectively; the result was similar to the dispersion polymerization of *t*BA. The number-average molecular weight (M_n) and polydispersity (M_w/M_n) of P*t*BA are shown in Fig. 7. The number-average molecular weight (M_n) linearly increased with the monomer conversion. As shown in Fig. 8, GPC traces for the polymerization of *t*BA took the form of single peak curves and were reasonably symmetrical. These results demonstrated the living character and controllability of (TMOP)Co(II) in the soap-free emulsion polymerization of *t*BA. It can be seen that the polymerization of *t*BA is observed to be controlled in the soap-free emulsion polymerization.

Table 4 Soap-free emulsion polymerizations of tBA mediated by (TMOP)Co(II)[a]

Run	$[t\text{BA}]_0/[\text{Co}]_0/[\text{VA-044}]$	Time (min)	Conv.[b] (%)	$M_{\text{n,th}}$[c] ($\times 10^4$)	$M_{\text{n,GPC}}$[d] ($\times 10^4$)	M_w/M_n
1	2000/1/3	50	40.0	10.2	1.45	2.08
2	2000/1/3	60	51.2	13.1	3.64	1.98
3	2000/1/3	70	55.4	14.2	7.61	2.16
4	2000/1/3	80	60.0	15.4	8.16	1.99
5	2800/1/3	50	30.2	10.8	3.72	1.93
6	2800/1/3	60	37.7	13.5	4.21	2.06
7	2800/1/3	70	42.0	15.1	6.25	1.47
8	2800/1/3	80	50.7	18.2	8.94	3.07
9	2800/1/3	100	55.3	19.8	11.5	3.42
10	3700/1/3	40	18.7	8.90	5.96	1.54
11	3700/1/3	60	31.7	15.0	19.1	2.38
12	3700/1/3	70	36.7	17.4	23.5	2.01
13	3700/1/3	80	45.5	21.6	31.6	2.11

[a] $[t\text{BA}]_0 = 10\%$; [Co] = [(TMOP)Co(II)]; c(SDS) = 0.006 mol L^{-1}; m(NaCl) = 0.05 g; $V_{\text{EtOH}}/V_{\text{H}_2\text{O}} = 2/8$; temperature, 50 °C. [b] The monomer conversion was determined by gravimetric analysis. [c] $M_{\text{n,th}} = M_{\text{w}(t\text{BA})} \times \text{ratio} \times \text{conv}$ (%). [d] Determined by gel permeation chromatography (GPC) calibrated by poly(MMA) standards.

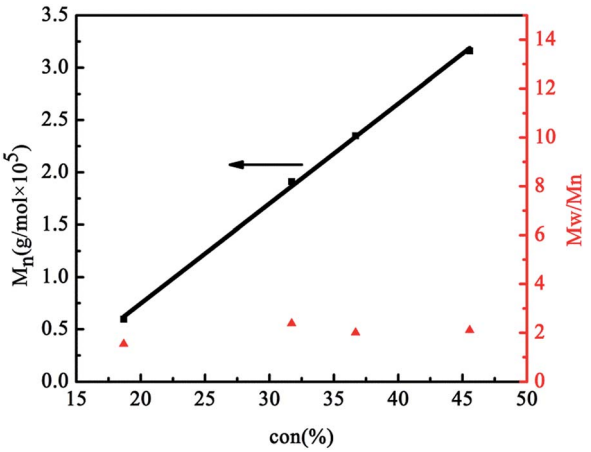

Fig. 7 Evolution of molar mass and polydispersity *versus* *t*BA conversion in the soap-free emulsion polymerization (conditions: $[tBA]_0/[Co]_0/[VA\text{-}044]_0$ = 3700/1/3; monomer, 10 wt%; *c*(SDS) = 0.006 mol L^{-1}; *m*(NaCl) = 0.05 g; V_{EtOH}/V_{H_2O} = 2/8; temperature, 50 °C).

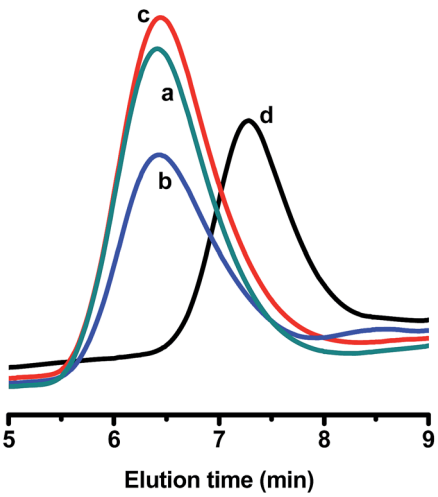

Fig. 8 GPC traces of P*t*BA, (a) Con. = 45.5%, $M_n = 31.6 \times 10^4$; (b) Con. = 36.7%, $M_n = 23.5 \times 10^4$; (c) Con. = 31.7%, $M_n = 19.1 \times 10^4$; and (d) Con. = 18.7%, $M_n = 5.96 \times 10^4$; (conditions: $[tBA]_0/[Co]_0/[VA\text{-}044]_0$ = 3700/1/3; monomer, 10 wt%; *c*(SDS) = 0.006 mol L^{-1}; *m*(NaCl) = 0.05 g; V_{EtOH}/V_{H_2O} = 2/8; temperature, 50 °C).

Herein, the morphology of the spherical and uniform particles in the soap-free emulsion polymerization was demonstrated using optical microscopy (Fig. 9a),[40] rather than scanning electron microscopy (SEM) or transmission electron microscopy (TEM) techniques because the latex needs to be dried before using the SEM or TEM technique to image the P*t*BA particles. From Fig. 9b, we can clearly see that the morphology of the dried particles appears to deform compared to that of the particles in the aqueous solution.

Experiments were conducted to investigate the effects of the SDS concentration, NaCl, and alcohol/water volume ratio on the particle size in the soap-free emulsion polymerization of *t*BA. The data are all shown in Tables 5–7 and Fig. 10–12. It can be

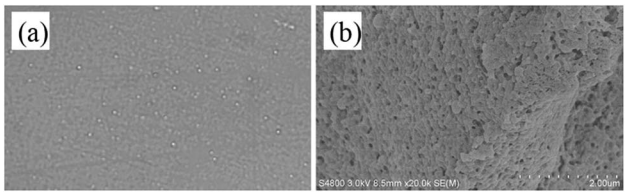

Fig. 9 Morphologies of P*t*BA particles demonstrated using (a) an optical microscope and (b) a scanning electron microscope (conditions: $[tBA]_0/[Co]_0$ = 3700/1; monomer, 10 wt%; *c*(SDS) = 0.006 mol L^{-1}; *m*(NaCl) = 0.05 g; V_{EtOH}/V_{H_2O} = 2/8; temperature, 50 °C).

Table 5 Effect of different amounts of SDS on the P*t*BA particle size

$[tBA]_0/[Co]_0/[VA\text{-}044]$	Solvent	*c*(SDS) (mol L^{-1})	D_{mean} (nm)
3700/1/3	V_{EtOH}/V_{H_2O} = 2/8	0.004	298.2
3700/1/3	V_{EtOH}/V_{H_2O} = 2/8	0.005	202.0
3700/1/3	V_{EtOH}/V_{H_2O} = 2/8	0.006	100.7

Table 6 Effect of different amounts of NaCl on the P*t*BA particle size

$[tBA]_0/[Co]_0/[VA\text{-}044]_0$	Solvent	*m*(NaCl/g)	D_{mean} (nm)
3700/1/3	V_{EtOH}/V_{H_2O} = 2/8	0.03	59.6
3700/1/3	V_{EtOH}/V_{H_2O} = 2/8	0.05	100.2
3700/1/3	V_{EtOH}/V_{H_2O} = 2/8	0.07	374.1

Table 7 Effect of V_{EtOH}/V_{H_2O} on the soap-free emulsion polymerization of *t*BA

$[tBA]_0/[Co]_0/[VA\text{-}044]$	Solvent	D_{mean} (nm)
3000/1/3	$V_{EtOH} : V_{H_2O}$ = 0 : 10	255.3
3000/1/3	$V_{EtOH} : V_{H_2O}$ = 1 : 9	241.3
3000/1/3	$V_{EtOH} : V_{H_2O}$ = 2 : 8	100.7
3000/1/3	$V_{EtOH} : V_{H_2O}$ = 3 : 7	80.6

seen from Table 5 and Fig. 10 that the final particle size decreased with the increasing concentration of SDS. It should be noted from the previous studies that some mechanisms other than micelle nucleation must be responsible for the particle formation process when the surfactant concentration is below the critical micelle concentration (CMC). For example, Priest,[41] Roe,[42] and Fitch and Tsai[43] proposed the homogeneous nucleation mechanism for the formation of particle nuclei in the continuous aqueous phase. The surfactant species required to stabilize the primary particles originate from those dissolved in the aqueous phase and those adsorbed on the monomer droplet surfaces. The amount of coagulum was greatly reduced by increasing the level of SDS.

Fig. 11(a) indicates the conversion–time curves for *t*BA at different concentrations of NaCl. It was observed that the higher the electrolyte concentration, the lower the rate of polymerization, which was also reported by other groups.[46,47] However, the particle size was enlarged with the concentration of NaCl, as

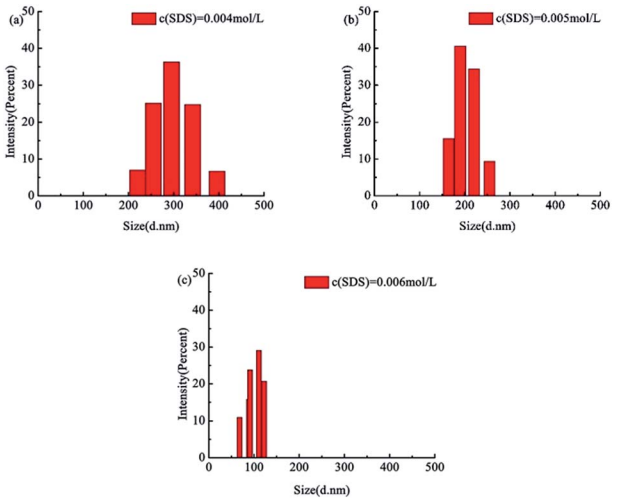

Fig. 10 Effect of SDS content on the P*t*BA microspheres' particle size distribution in the soap-free emulsion polymerization (a) c(SDS) = 0.004 mol L^{-1}, (b) c(SDS) = 0.005 mol L^{-1}, and (c) c(SDS) = 0.006 mol L^{-1} (conditions: $[tBA]_0/[Co]_0$ = 3700/1; monomer, 10 wt%; m(NaCl) = 0.05 g; V_{EtOH}/V_{H_2O} = 2/8; temperature, 50 °C).

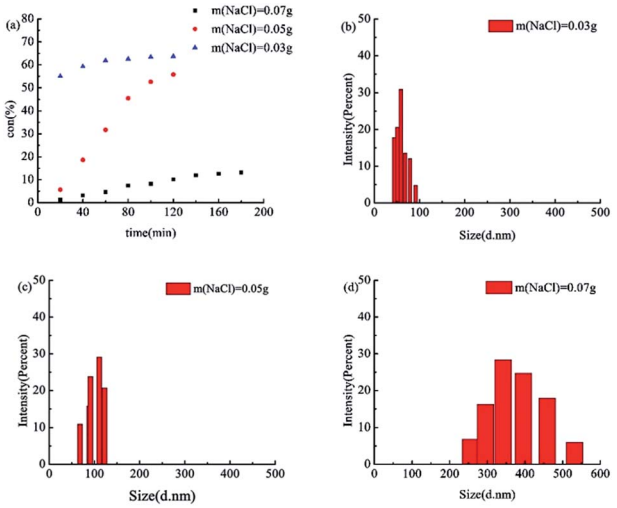

Fig. 11 Effect of NaCl content on the monomer conversion rate and P*t*BA microspheres' particle size distribution in the soap-free emulsion polymerization. (a) Evolution of *t*BA conversion *versus* time at different NaCl contents, (b) m(NaCl) = 0.03 g, (c) m(NaCl) = 0.05 g, and (d) m(NaCl) = 0.07 g (conditions: $[tBA]_0/[Co]_0$ = 3700/1; monomer, 10 wt%; c(SDS) = 0.006 mol L^{-1}; V_{EtOH}/V_{H_2O} = 2/8; temperature, 50 °C).

shown in Table 6 and Fig. 11(b)–(c). Because the concentration of NaCl was higher, the stability of the particles decreased through compressing the electric double layer, resulting in the occurrence of particle coagulation. The coagulation of the particles promoted a rapid increase in the particle size.[44,45]

The effect of the alcohol to water ratio (V_{EtOH}/V_{H_2O}) on the P*t*BA particles was also studied. As is shown in Table 7 and Fig. 12, the result demonstrated that the particle size decreased with the increased value of V_{EtOH}/V_{H_2O}, which is just opposite to the result of methyl methacrylate (MMA)[48] because MMA can dissolve well in alcohol; however, *t*BA is barely soluble.

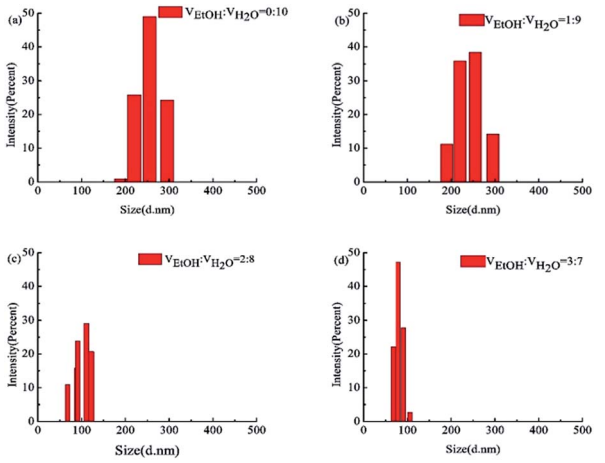

Fig. 12 Size distribution of the particles of P*t*BA in the soap-free emulsion polymerization (a) $V_{EtOH} : V_{H_2O}$ = 0 : 10, (b) $V_{EtOH} : V_{H_2O}$ = 1 : 9, (c) $V_{EtOH} : V_{H_2O}$ = 2 : 8, and (d) $V_{EtOH} : V_{H_2O}$ = 3 : 7 (conditions: $[tBA]_0/[Co]_0$ = 3700/1; monomer, 10 wt%; c(SDS) = 0.006 mol L^{-1}; m(NaCl) = 0.05 g; temperature, 50 °C).

Conclusions

The cobalt porphyrin (TMOP)Co(II)-mediated living radical polymerization of *t*BA was successfully carried out in the dispersion and soap-free emulsion polymerization. The number-average molecular weight linearly increased with the monomer conversion. In the dispersion polymerization system, the particle size decreased with the increasing PVP concentration and $[tBA]_0/[Co]_0$. Furthermore, the P*t*BA particle sizes obtained from the soap-free emulsion polymerization system were less than 300 nm with relatively low polydispersity. In addition, the particle sizes decreased with the increasing concentration of SDS and V_{EtOH}/V_{H_2O} value; simultaneously, the particle sizes enlarged with the increasing NaCl content. Thus, the environmentally friendly emulsion polymerization process using the LRP technique is worthwhile in preparing P*t*BA particles with the targeted molecular weight and in high conversion. Moreover, further study is currently ongoing to combine the living radical dispersion and soap-free emulsion polymerization mediated by other cobalt complexes such as (selen)Co(II), and so on, to prepare uniform spherical particles.

Acknowledgements

This work was financially supported by the National Science Foundation for Young Scientists of China (No. 21302083 and 51562029), the Teaching Reform Project of Inner Mongolia University of Technology (No. 2014212 and 2014217), and the Program of Natural Science Foundation of Inner Mongolia University of Technology, China (No. X201503). The authors thank the Institute of Coal Conversion and Cyclic Economy for their support in carrying out these experiments. The authors also thank Professor Xuefeng Fu of Peking University for her helpful discussion.

Notes and references

1 Y. Kim, K. Kim, B. H. Lee and S. Choe, *Macromol. Res.*, 2012, **20**(9), 977–984.
2 X. G. Li, M. R. Huang, J. F. Zeng and M. F. Zhu, *Colloids Surf., A*, 2004, **248**(1), 111–120.
3 X. G. Li, H. J. Zhou and M. R. Huang, *Polymer*, 2005, **46**(5), 1523–1533.
4 E. Makarewicz, *Prog. Org. Coat.*, 1997, **31**(3), 217–222.
5 F. Candau and P. Buchert, *Colloids Surf.*, 1990, **48**, 107–122.
6 G. Moad, E. Rizzardo and S. H. Thang, *Acc. Chem. Res.*, 2008, **41**(9), 1133–1142.
7 S. M. Kimani and S. C. Moratti, *Macromol. Rapid Commun.*, 2006, **27**(22), 1887–1893.
8 Y. Zhao, S. Zhang, Z. Wu, X. Liu, X. Zhao, C.-H. Peng and X. Fu, *Macromolecules*, 2015, **48**, 5132–5139.
9 C. Boyer, V. Bulmus, T. P. Davis, V. Ladmiral, J. Liu and S. Perrier, *Chem. Rev.*, 2009, **109**, 5402–5436.
10 C. Boyer, N. A. Corrigan, K. Jung, D. Nguyen, T.-K. Nguyen, N. N. M. Adnan, S. Oliver, S. Shanmugam and J. Yeow, *Chem. Rev.*, 2016, **116**, 1803–1949.
11 K. Matyjaszewski and J. Xia, *Chem. Rev.*, 2001, **101**(9), 2921–2990.
12 D. Benoit, V. Chaplinski, R. Braslau and C. J. Hawker, *J. Am. Chem. Soc.*, 1999, **121**, 3904–3920.
13 C. J. Hawker, A. W. Bosman and E. Harth, *Chem. Rev.*, 2001, **101**, 3661–3688.
14 M. Hurtgen, C. Detrembleur, C. Jerome and A. Debuigne, *Polym. Rev.*, 2011, **51**(2), 188–213.
15 L. E. N. Allan, M. R. Perry and M. P. Shaver, *Prog. Polym. Sci.*, 2012, **37**(1), 127–156.
16 A. Debuigne, R. Poli, C. Jérôme, R. Jérôme and C. Detrembleur, *Prog. Polym. Sci.*, 2009, **34**(3), 211–239.
17 B. B. Wayland, G. Poszmik, S. L. Mukerjee and M. Fryd, *J. Am. Chem. Soc.*, 1994, **116**, 7943–7944.
18 B. B. Wayland, L. Basickes, S. Mukerjee and M. Wei, *Macromolecules*, 1997, **30**(26), 8109–8112.
19 C. H. Peng, M. Fryd and B. B. Wayland, *Macromolecules*, 2007, **40**, 6814–6819.
20 Z. Lu, M. Fryd and B. B. Wayland, *Macromolecules*, 2004, **37**, 2686–2687.
21 B. B. Wayland, C. H. Peng, X. Fu, Z. Lu and M. Fryd, *Macromolecules*, 2006, **39**, 8219–8222.
22 S. Li, B. Bruin, C. H. Peng, M. Fryd and B. B. Wayland, *J. Am. Chem. Soc.*, 2008, **130**(40), 13373–13381.
23 Y. Zhao, H. Dong, Y. Li and X. Fu, *Chem. Commun.*, 2012, **48**(29), 3506–3508.
24 Y. Zhao, M. Yu, S. Zhang, Y. Liu and X. Fu, *Macromolecules*, 2014, **47**(18), 6238–6245.
25 Y. Zhao, M. Yu and X. Fu, *Chem. Commun.*, 2013, **49**(45), 5186–5188.
26 L. Wang, H. Zhao, B. Wang, J. Sun, Y. Zhang, L. Ji and Z. Cao, *RSC Adv.*, 2016, **6**(68), 63519–63524.
27 H. Zhu, M. L. Du, M. L. Zou, C. S. Xu, N. Li and Y. Q. Fu, *J. Mater. Chem.*, 2012, **22**, 9301–9307.
28 X. Su, Z. Zhao, H. Li, X. Li, P. Wu and Z. Han, *Eur. Polym. J.*, 2008, **44**(6), 1849–1856.
29 P. E. Millard, N. C. Mougin, A. Böker and A. H. E. Müller, *ACS Symp. Ser.*, 2009, **1203**, 127–137.
30 A. Anastasaki, A. J. Haddleton, Q. Zhang, A. Simula, M. Droesbeke, P. Wilson and D. M. Haddleton, *Macromol. Rapid Commun.*, 2014, **35**(10), 965–970.
31 Q. Zhang, P. Wilson, Z. Li, R. McHale, J. Godfrey, A. Anastasaki, C. Waldron and D. M. Haddleton, *J. Am. Chem. Soc.*, 2013, **135**(19), 7355–7363.
32 Y. Li and B. B. Wayland, *Chem. Commun.*, 2003, **13**, 1594–1595.
33 J. Qiu, B. Charleux and K. Matyjaszewski, *Prog. Polym. Sci.*, 2001, **26**(10), 2083–2134.
34 H. Kaneyoshi and K. Matyjaszewski, *Macromolecules*, 2005, **38**(20), 8163–8169.
35 M. Hurtgen, J. Liu, A. Debuigne, C. Jerome and C. Detrembleur, *J. Polym. Sci., Part A: Polym. Chem.*, 2012, **50**(2), 400–408.
36 C.-M. Liao, C.-C. Hsu, F.-S. Wang, B. B. Wayland and C.-H. Peng, *Polym. Chem.*, 2013, **4**(10), 3098–3104.
37 A. J. Paine, W. Luymes and J. McNulty, *Macromolecules*, 1990, **23**(12), 3104–3109.
38 S. Shen, E. D. Sudol and M. S. El-Aasser, *J. Polym. Sci., Part A: Polym. Chem.*, 1993, **31**(6), 1393–1402.
39 C. M. Tseng, Y. Y. Lu, M. S. El-Aasser and J. W. Vanderhoff, *J. Polym. Sci., Part A: Polym. Chem.*, 1986, **24**(11), 2995–3007.
40 Y. Zou, Y. H. Zhang and P. X. He, *Des. Monomers Polym.*, 2013, **16**(6), 592–600.
41 W. J. Priest, *J. Phys. Chem.*, 1952, **56**(9), 1077–1082.
42 C. P. Roe, *Ind. Eng. Chem.*, 1968, **60**(9), 20–33.
43 R. M. Fitch and C. H. Tsai, *Polymer Colloids*, Springer, US, 1971, pp. 73–102.
44 T. Yamamoto, *Colloid Polym. Sci.*, 2012, **290**(11), 1023–1031.
45 X. Xu, B. Liu, M. Zhang, S. Liu, F. Zhu and J. Wang, *J. Polym. Res.*, 2016, **23**(1), 1–9.
46 F. Jahanzad, *J. Appl. Polym. Sci.*, 2010, **117**(1), 84–90.
47 A. S. Dunn and Z. F. M. Said, *Polymer*, 1982, **23**(8), 1172–1176.
48 D. Wang, B. Liu and J. Hu, *Polym. Mater.: Sci. Eng.*, 2004, **6**, 109–112.